

Ca²⁺ signalling is critical for autoantibody-induced blistering of human epidermis in pemphigus vulgaris

Thomas Schmitt¹, Desalegn Egu¹, Elias Walter¹, Anna Sigmund¹, Ramona Eichkorn², Amir Yazdi², Enno Schmidt³, Miklós Sárdy⁴, Ruediger Eming⁵, and Jens Waschke¹

¹Ludwig-Maximilians-Universität München Anatomische Anstalt

²University Medical Center Tübingen Pharmacy

³University of Lübeck

⁴Semmelweis University

⁵Philipps-Universität Marburg

September 16, 2020

Abstract

Background: Pemphigus vulgaris (PV) is a severe autoimmune skin disease. Autoantibodies in PV (PV-IgG) targeting desmoglein (DSG)1 are required for loss of desmosome adhesion and skin blistering. Objectives: The aim was to connect the single steps of a Ca²⁺ flux dependent pathway and show it's importance for the pathogenesis of pemphigus vulgaris. Methods: Applied methods include immunoprecipitation, Ca²⁺-flux analysis with FURA2-AM, analysis of protein phosphorylation with Western-blotting, Immunofluorescence, investigation of loss of adhesion in dissociation assays and human skin ex-vivo blistering model. Results: PV-IgG but not a DSG3-specific monoclonal antibody (AK23) caused Ca²⁺ influx in primary human keratinocytes. Phosphatidylinositol 4 kinase- α (PI4K) interacts with DSG1 but not DSG3. Its downstream targets, phospholipase-C- γ 1 (PLC) and protein-kinase-C α , similar to p38MAPK interacted with both. PLC was activated by PV-IgG but not by AK23. PLC regulates the release of Inositol-1,4,5-trisphosphate (IP3) causing IP3-receptor (IP3R) activation and Ca²⁺ flux from the endoplasmic reticulum into the cytosol. This stimulates Ca²⁺-release-activated-channels (CRAC) causing Ca²⁺ influx. Inhibitors against PI4K, PLC, IP3R or CRAC effectively blocked PV-IgG-induced Ca²⁺ influx and ameliorated alterations of DSG1 and 3 localization, keratin filament retraction, actin disruption and loss of cell adhesion in vitro. Moreover, inhibiting PLC was protective against blister formation, redistribution of DSG1 and 3 and actin disruption in human skin ex vivo. Conclusions: These results demonstrate that Ca²⁺-mediated signalling is important for pemphigus pathology and dependent on the autoantibody profile, with different roles for the Dsg1 and Dsg3 complexes. PLC could be an interesting pharmaceutical target.

INTRODUCTION

The skin as the main outer barrier against pathogens, chemicals and other hazards is an important organ. The autoimmune disease pemphigus vulgaris (PV) affects the mucosa and epidermis. Disruption of the skin barrier, caused by often extensive blisters, can lead to severe complications and high mortality if untreated. Current first-line treatments are systemic high-dose long term corticosteroids with or without further immunosuppressants or rituximab combined with rapidly tapered corticosteroids, both associated with high rates of severe adverse events. Other treatment options such as intravenous-immunoglobulin G (IV-IgG) or immuno-adsorption also have drawbacks, including availability of donor IgG, immunosuppressive effects and short-term effectiveness. Understanding the mechanisms of PV pathology and finding specific treatment options are thus the main goals of current research.

PV is caused by autoantibodies (PV-IgG) including IgG against the desmosomal proteins desmoglein (*DSG*

)1 and 3 and autoantibodies against other target proteins . Desmosomes are adhesive cell-cell contacts in the epidermis , in which *DSG* s are connected to plaque proteins including desmoplakin (*DP*) which links them to the keratin cytoskeleton .

Desmosomes provide mechanical stability, but also partake in cellular signalling . In pemphigus, loss of desmosomal adhesion is caused by both direct inhibition of *DSG* binding and cellular signalling mechanisms .

It is well-known that the clinical phenotype of PV correlates with the autoantibody profile and anti-*DSG* 1-IgG are believed to be required for epidermal blistering . It is thus possible that anti-*DSG* 1-IgGs modulate specific signalling pathways involved in loss of desmosomal adhesion . Indeed, Ca^{2+} influx in human keratinocytes was shown to be induced by PV-IgG including autoantibodies against *DSG* 1 but not by AK23, a*DSG* 3-specific IgG . PV-IgG is known to lead to activation of phospholipase-C γ 1 (*PLC*) generating inositol-1,4,5-trisphosphat (IP3) and increasing the intracellular Ca^{2+} concentration . In line with this, an interaction between *DSG* 1 and *PI4K* (phosphoinositole-4-kinase α), upstream of *PLC* , was predicted .

Further downstream, IP3 activates *IP3R*(Inositol-trisphosphate-receptor), releasing Ca^{2+} from the endoplasmic reticulum (ER) into the cytosol . Ca^{2+} flux from the ER into the cytosol stimulates Ca^{2+} -release-activated-channels (CRAC) causing further Ca^{2+} influx . Ca^{2+} activates protein kinase-C α (*PKC*) , which was shown to also be important for PV-IgG-induced loss of keratinocyte adhesion and skin blistering by mechanisms including depletion of *DSG* 3 , keratin retraction and loss of cell adhesion *in vitro* and in mice *in vivo* .

RESULTS

PV-IgG induces DSG1-dependent Ca^{2+} flux via IP3R and CRAC in vitro

IP3R is required to redistribute Ca^{2+} from the ER to the cytosol but not sufficient to increase intracellular Ca^{2+} concentrations. To achieve this, *STIM1* and *ORAI1* form the so-called CRAC (Ca^{2+} -release-activated-channel), in which *STIM1* serves as a Ca^{2+} concentration sensor at the ER membrane . Upon low Ca^{2+} , *STIM1* contacts *ORAI1* at the plasma membrane to replenish the ERs Ca^{2+} store . We found *IP3R* and *ORAI1* to be equally distributed in all epidermal layers, whereas *STIM1* immunostaining was more prominent in the granular layer (Figure 1a). Similar to previous studies , PV-IgG containing autoantibodies against *DSG* 1 and *DSG* 3 (Table 1) but not IgG from healthy volunteers led to an increase in intracellular Ca^{2+} in NHEK cells (Figure 1b/S1a). In agreement with a previous report , the Ca^{2+} flux was anti-*DSG* 1-dependent, as no influx was observed for the anti-*DSG* 3-mAb AK23 (Figure 1b/S1a). Inhibition of CRAC with BTP-2, *IP3R* with Xestospongin C (Xest), *PLC* with U-73122 or *PI4K* with GSK-F1 abolished the Ca^{2+} flux (Figure 1b/S1a). Co-immunoprecipitation demonstrated that *PI4K* interacts with *DSG* 1 but not with *DSG* 3, *DSG* 1 s downstream target *PLC* as well as *p38MAPK* (Figure 1c+d/S1b), which is known to be strongly involved in PV pathogenesis , are part of both complexes. So far, only the interaction of *p38MAPK* with *DSG* 3 was shown . Phosphorylated *PKC* , reported to be responsible for the cytoskeleton reorganization and *DSG* 3 depletion , was found in both complexes (Figure 1c+d). PV-IgG but not AK23 induced phosphorylation of *PLC* (Figure 1e+f). Taken together, these results demonstrate that a *DSG* 1-specific complex exists which, induced by PV-IgG, can initiate a Ca^{2+} flux dependent pathway.

Inhibition of Ca^{2+} flux is protective against PV-IgG-induced pathogenic effects in vitro

PV-IgG caused loss of keratinocyte adhesion in dispase-based dissociation assays. Treatment with inhibitors against *PI4K* , *PLC* , *IP3R* or CRAC added 1 h before PV-IgG effectively blocked cell monolayer fragmentation after 2 h and 24 h. After 24 h, inhibition of *PLC* was the most effective and even reduced the effect of AK23 (Figure 2a-d/S2a-d).

The role of Ca^{2+} signalling for PV-IgG-mediated effects on *DSG* 1 and *DSG* 3 localization, keratin retraction and reorganization of cortical actin was assessed by immunostaining and F-actin staining. After 24 h of PV-IgG treatment, *DSG* 1 and *DSG* 3 immunostaining was fragmented at cell borders and partially relocated

to the cytosol. Treatment with inhibitors for *PI4K*, *PLC*, *IP3R* or CRAC, ameliorated pathogenic effects (Figure 3a/S3a-c).

Retraction of keratin filaments from the cell borders was visible after 24 h of PV-IgG treatment. Treatment with the inhibitors ameliorated the effect (Figure 3b/S3d). Similarly, cortical F-actin also showed defects especially close to intercellular gaps after PV-IgG treatment, which was ameliorated by the respective inhibitors (Figure 3/S3). F-actin staining was more pronounced following inhibition of *PLC* compared to controls (Figure 3/S3) indicating that *PLC* basal activity might regulate actin remodelling.

Inhibition of Ca²⁺ flux is protective against PV-IgG-induced pathogenic effects in human skin ex vivo

In human skin samples PV-IgG induced blistering (Figure 4a) where typical tombstoning was observed (Figure 4/S4). At the blistering sites, PV-IgG was enriched and in non-affected regions it was deposited at cell borders (Figure S4a). *DSG 1* and *3* staining was fragmented and redistributed to the cytosol in response to incubation with autoantibodies (Figure 4c/S4b). Moreover, actin staining was almost abolished at blistering sites (Figure 4d). All pathogenic effects were completely blocked by inhibition of *PLC* (Figure 4/S4). This demonstrates that *PLC* is important for PV-IgG-induced blistering of human skin.

DISCUSSION AND CONCLUSION

The roles of Ca²⁺ influx and PLC for pemphigus vulgaris pathogenesis

Ca²⁺ flux-dependent signalling plays an important role in pemphigus pathogenesis. Inhibiting Ca²⁺ signalling blocks PV-IgG-induced loss of keratinocyte adhesion *in vitro* and blistering in human skin *ex vivo* (Figure 5). Binding of PV-IgG to *DSG 1* [1], associated with *PI4K* and *PLC*, activates *PLC* and releases IP3 [2]. IP3 activates *IP3R* thereby releasing Ca²⁺ from the ER into the cytosol [3]. Low ER Ca²⁺ concentration activates *STIM1* at the ER membrane. *STIM1* contacts *ORAI1* by forming the CRAC and thereby causing Ca²⁺ influx from the extracellular space [4]. With the *IP3R* still active, this further increases the Ca²⁺ concentration in the cytosol. Cytosolic Ca²⁺ finally activates *PKC* [5], which destabilizes the desmosome by keratin retraction and depletion of *DSG 1* and *DSG 3* [6].

The complete mechanism of action of *PKC* is still unknown. However, it presumably affects desmosome turnover on several levels. Upon PV-IgG treatment *PKC* has been proposed to translocate to the desmosomal plaque. Cytoskeletal components such as keratin 8 and 18 are substrates of *PKC* possibly inducing keratin filament retraction. Similarly, *PKC* affects the actin cytoskeleton, mostly causing disassembly and reduced anchorage and may also modulate desmosome turn-over by modulating the actin-binding adducin. Moreover, *PKC* phosphorylates *DP* which is involved in destabilizing the desmosome, and caused *DSG 3* fragmentation and acantholysis in pemphigus passive-immune-transfer mouse models which supports the observations that inhibiting *PKC* ameliorated PV-IgG-induced loss of adhesion *in vitro*.

Ca²⁺ has very profound effects on desmosome regulation. The stability of newly formed desmosomes is dependent on extracellular Ca²⁺. After several days, desmosomes become hyper-adhesive and independent of extracellular Ca²⁺. Hyper-adhesive desmosomes are also less sensitive to PV-IgG. Inhibiting *PKC* causes a rapid transformation from Ca²⁺-dependent to Ca²⁺-independent desmosomes. Active *PKC* is associated with *DSG 1*, which is known to be important for regulation of epidermal differentiation. It is thus conceivable that *DSG 1* controls desmosome adhesion and skin differentiation at least in part by controlling Ca²⁺ levels in keratinocytes.

Loss of cell adhesion in response to AK23, which did not cause Ca²⁺ influx and disrupts *DSG 3* but not *DSG 1* was ameliorated significantly by inhibiting *PLC*. This indicates that *PKC*, which was observed to be involved in *DSG 3* depletion *in vivo* and *in vitro* may be activated independently of Ca²⁺ or baseline activity is sufficient. It was reported, that PV-IgG against thyroid peroxidase and other targets might also be able to activate Ca²⁺ flux possibly via *PLC*. This indicates that these non-desmoglein antibodies might play a crucial role for disease severity and relapse.

It is unlikely that *PKC* is the sole downstream pathway activated by antibodies against *DSG 1*. In human

epidermis, inhibition of *PKC* alone under conditions which were effective *in vitro* and in mice *in vivo*, was not enough to block blistering in human skin *ex vivo*. In contrast, inhibition of *p38MAPK*, was protective in murine skin *in vivo* and human epidermis but not in mucosa *ex vivo*. Since we observed that *p38MAPK* is associated with both *DSG 1* and *DSG 3*, these data are compatible with the hypothesis that antibodies against *DSG 1* and *DSG 3* or other targets are required for skin blistering. *PLC* might also modulate other events regulated by *p38MAPK* such as actin remodelling via *RHOA*.

This demonstrates that PV pathology is dependent on the antibody profiles, different anti-*DSG 1/DSG 3* ratios as well as different target epitopes might play an important role. This might influence the clinical phenotype by inducing specific signalling responses in keratinocytes. More studies are required to delineate the functional interplay between the complex mechanisms involved in pemphigus pathogenesis. Nevertheless, the data presented here can explain for the first time why autoantibodies against *DSG 1* but not *DSG 3* are required for epidermal involvement in PV. Since *PI4K* upstream of Ca^{2+} signalling specifically interacts with *DSG 1* but not with *DSG 3*, this knowledge may allow a new strategy to develop *DSG 1*-specific treatment options in pemphigus.

MATERIALS & METHODS

Cell Culture

For all *in vitro* experiments, primary normal human epithelial keratinocytes (NHEK) in passage 3-6 were used. NHEKs were generated at the Universitäts-Hautklinik Tübingen, approved by the medical ethical committee of the Eberhard Karls University Tübingen (ethical approval: 547/2011BO2). The cells were isolated from juvenile foreskin derived from patients, who have given written informed consent. The epidermis was isolated using 50 mg/ml dispase II (Roche, Switzerland). Cells were separated using a trypsin-EDTA solution (Merck, Germany). The cells were cultivated in a humidified, 5 % CO_2 atmosphere at 37 °C in CnT-07 medium (CELLnTEC, Switzerland) containing 10 µg/ml gentamycin and 0.25 µg/ml amphotericin B. The cells were kept under low calcium conditions (0.06 mM Ca^{2+}). 24 h prior to treatment, the confluent cells were differentiated by adding 1.8 mM Ca^{2+} . For experiments the cells were incubated with vehicle or mediators 1:50 in DMSO with final concentrations: CRAC inhibitor BTP-2 (Merk, Germany), 10 µM; *PI4K* inhibitor GSK-F1 (SYNkinase, Australia), 10 nM; *PLC* inhibitor U-73122 (Santa Cruz, USA), 4 µM; or *IP3R* inhibitor Xestospongin C (Abcam, USA), 2 µM for 1 h before IgG treatment.

Patient IgGs

[Table1]

Immunostaining

Cells were grown on glass coverslips and fixed with 2 % paraformaldehyde for 5 min (for rabbit-anti-*DSG 3*-mAb (Biozol, Germany), rabbit-anti-*DSG 1*-pAb (Abclonal, USA), mouse-anti-*DSG 1*-mAb (Progen, Germany) mouse-anti-GAPDH-mAb (Santa Cruz, USA), mouse-anti-HSP60-mAb (Thermo Scientific, USA) rabbit-anti-*IP3R* -pAb (Abcam, USA), mouse-anti-Orai1-mAb (Santa Cruz, USA), rabbit-anti-*PI4K* α-mAb (Abxexa, United Kingdom), rabbit-Anti-p-*PKC* α-mAb (Abcam, USA), rabbit-anti-p-*PLC* γ1-mAb (Cell signaling, USA), rabbit-anti-Stim1-mAb (Cell signaling, USA) and in ethanol (-20 °C) shaking on ice for 30 min and acetone (-20 °C) for 3 min (For mouse-anti-cytokeratin-pan-mAb (Sigma Aldrich, USA) 1:100-200. Paraformaldehyde fixed cells were permeabilized with 1 % Triton X-100 in PBS for 5 min (for acetone fixed cells no permeabilization was necessary), the cells were blocked with 3 % bovine serum albumin (BSA) and 1 % normal goat serum in PBS for 30 min. Primary antibodies were applied overnight at 4 °C. Cy3 coupled goat-anti-rabbit/mouse/human secondary antibodies (Dianova, Germany) and Alexa-488-phalloidin (Life technologies, USA) were incubating for 1 h and DAPI 1:10.000 for 15 min. The cover slips were mounted with 2 % n-propyl-gallate and evaluated with a SP5.II confocal microscope with a 63x NA 1.4 PL APO objective (Leica, Germany). After heating to 60 °C for 30 min the skin slices were treated the same, except for 1 h permeabilization. The cells were washed 3x with PBS in between each step except ethanol to acetone.

Ratiometric intracellular Ca^{2+} measurements

Fura-2AM (Thermo Fisher, USA) was used to measure intracellular Ca^{2+} in real time. The cells were grown in an 8-well μ -slide (Ibidi, Germany). Mediators were contained in all incubation steps and during the measurement. A mix of 1 μM Fura-2AM and 0.02 % Pluronic (Thermo Fisher, USA) was applied for 20 min in measurement buffer (140 mM NaCl, 3.6 mM KCl, 2.6 mM $\text{CaCl}_2(\text{H}_2\text{O})_2$, 0.5 mM MgSO_4 , 0.5 mM $\text{NaH}_2\text{PO}_4(\text{H}_2\text{O})_2$, 2 mM NaHCO_3 , 5 mM HEPES and 5 mM D+Glucose, pH 7.35) at 37 °C. The cells were washed twice with measurement buffer. Measurements were performed using MetaFluor (Moleculardevices, USA) on an Axio Observer A1 (Zeiss, Germany) with a Polychrome V (Till Photonics, Germany), a CoolSNAP-Hq2 digital camera (Photometrics, USA) and a Fura-2 filter set.

Co-Immunoprecipitation

NHEK were cultured in T75-Cell flasks, washed 1x with PBS +10 g/l EDTA and 2x with PBS. 1 ml Ca^{2+} -free-PBS with $\frac{1}{2}$ NaCl concentration +1 % triton-X100 +1 % Nonoxinol-40 +0.1 % sodium-dodecyl-sulfate +cOmplete (Merk, USA) was used for cell lysis shaking 15 min on ice. Buffer without SDS, 0.5 % Triton-X100 and 0.1 % Nonoxinol-40 was used for washing. The cells were mechanically detached and sheared with a 5 ml syringe and 10G needle (B.Braun, Germany) 10x. The resulting suspension was centrifuged at 4 degC for 15 min at 13.000 rpm and the pellet was removed. The protein amount was determined with a commercial Pierce BCA protein assay kit. The supernatant was added to buffer-washed Agarose G beads (Milipore, USA) adding about 600-1000 μg /protein. After 1.5 h on a rotator, the beads were removed via centrifuging for 2 min at 4 °C, 8.000 rpm and the supernatant was mixed with 1.5 μl of antibody or normal rabbit IgG, 1 mM Ca^{2+} and 0.5 mM Mg^{2+} and rotated for 3 h. The mixture was added to washed beads and rotated at 4 °C over night. The beads were washed 3x (1 min 4 °C, 3.000 rpm). Proteins were released from the beads using 27 μl 95 °C, 3x Lämmli-buffer and beads were removed by centrifuging (5 min 4 °C, 8.000 rpm).

Cell lysis, gel electrophoresis and Western blotting

Cells were cultured in 24-well-plates. Lysates were fractionated into a soluble cytosolic and insoluble cytoskeletal bound fraction using triton-extraction-buffer (0.5 % Triton X-100, 50 mmol/l MES, 25 mmol/l EGTA, 5 mmol/l MgCl_2 , pH 6.8, 0.1 % pepstatin+aprotinin+leupeptin, 1 % PMSF) for 10 min on ice under gentle shaking. The pellet=cytoskeletal fraction was separated at 14.000 rpm for 10 min at 4° C and the supernatant=cytosolic fraction was retrieved. The pellet was washed 1x and lysed with ultrasound in SDS lysis buffer (25 mM HEPES, 2 mM EDTA, 25 mM NaF, 1 % SDS, pH 7.6, cOmplete (Merk, USA)). Protein amount was determined with a commercial Pierce BCA protein assay kit. Western-blotting was performed, using a standard wet blotting protocol on nitrocellulose membranes (Life Technologies, USA). Membranes were blocked with ROTI(r)Block (Carl Roth, Germany) 1:10 in Tris-buffered saline with 0.05 % tween (TBST) for 1 h antibodies were used overnight at 4 degC in 5 % BSA in TBST 1:1000, except anti-p-*PKC* α (1:20.000). Anti-rabbit/mouse horseradish-peroxidase-coupled secondary antibodies (Dianova, Germany) were used 1:10.000 in TBST for 1 h and visualized with self-made ECL solution on a FluorchemE developer (Protein Simple, USA).

Dispase-based dissociation assay

After incubation, confluent cell monolayers were washed with Hank's buffered saline solution (HBSS) and subjected to 2.4 U/ml dispase II (Sigma Aldrich, USA) in HBSS for 20 min at 37 °C, 95 % humidity and 5 % CO_2 . After detachment of the monolayer the reaction was stopped by adding 200 μl HBSS. Defined shear stress was applied with an electrical pipette. Images for fragment counting were taken using a binocular microscope (Leica, Germany) and an EOS 600D camera (Canon, Japan).

Human skin samples

Skin biopsies were taken from body donors received by the Institute of Anatomy and Cell Biology, Ludwig-Maximilian-Universität München, Germany. Body donors had given written informed consent for use of tissue samples for research purposes. The procedure was approved by the Ethics Committee of the Faculty of Medicine (project no. 249-12). Only samples from body donors deceased for <24 h were used. Each

epidermis piece $\sim 4 \text{ cm}^2$ was excised from the shoulder region and divided into $\sim 1 \text{ cm}^2$ pieces.

Either 50 μl of the *PLC* -inhibitor U-73122, 4 μM in DMSO/PBS 1:50 or vehicle were injected intra-epidermally, followed by floating incubation in 5 ml Dulbecco's modified Eagle's medium, containing 10 % FCS, 50 U/ml penicillin and 50 mg/ml streptomycin, with the epidermis facing upwards at the liquid-air-interface without additional support at 95 % humidity, 5 % CO_2 and 37 °C. After 1 h incubation, either PV2 or IgG obtained from healthy volunteers, purified for experimental use by protein A affinity chromatography as described previously was injected. Injections were performed using a 0.01-1 ml syringe (B.Braun, Germany), and a 0.3x12 mm BL/LB 30Gx1/2" needle (B.Braun, Germany). After 24 h, shear stress was applied using a rubber piece. The skin pieces were cut and processed for either hematoxylin and eosin (H&E) or immunostaining.

H&E-staining

Samples were embedded in tissue freezing medium (Leica Biosystems, Germany) and 7 μm sections were made using a CryoStar NX70 Kryostat (Thermo Fisher, USA). The resulting sections were stained with H&E according to standard protocols. For morphometric analysis, images were captured at 200 \times magnifications using a light DMI8-Microscope (Leica, Germany).

Statistical analysis

Data were analysed in Excel (Microsoft, USA) and compared using one/two-way-ANOVA followed by Bonferroni-post-hoc-test (for Gaussian-distributed samples) using Graphpad Prism (Graphpad Software, USA). Error bars represent SEM. Significance was assumed with $p \leq 0.05$. Data are shown as mean \pm SEM. Each n represents one independent experiment.

Author contributions

Thomas Schmitt: Designing and conducting experiments, acquiring and analyzing data, writing the manuscript

Desalegn Egu: Conducting experiments

Elias Walter: Designing experiments, conducting preliminary experiments

Anna Sigmund: Contributing to experiment conduction

Ramona Eichkorn: Providing primary cells

Amir Yazdi: Providing primary cells

Enno Schmidt: Providing patient sera

Miklos Sardy: Providing patient sera

Rudiger Eming: Providing patient sera

Jens Waschke: Desingning experiments, analyzing data, writing the manuscript

Data Availability

The raw data supporting the conclusions of this manuscript will be made available by the authors, without undue reservation, to any qualified researcher.

Acknowledgements

We thank Silke Gotschy, Martina Hitzenbichler, and Sabine Muhlsimer for their excellent technical assistance as well as Jessica Plewa, Michael Becker, and Axel Unverzagt for assistance with human body donors. All PV samples were received from patients who had given written informed consent. A positive ethics vote was given for: PV1, University clinic Lubeck (Az 12-178), PV2 University Clinic Budapest (249-12), PV3 University Clinic Giessen/Marburg (Studie 20/14). All patients suffered from PV with mucocutaneous involvement.

The study was supported by DFG FOR 2497 to JW and AY and in part by structural funds of the Excellence Cluster Precision Medicine in Chronic Inflammation (EXC 2167) from the Deutsche Forschungsgemeinschaft to ES.

References

Table 1: PV-IgG used in this study

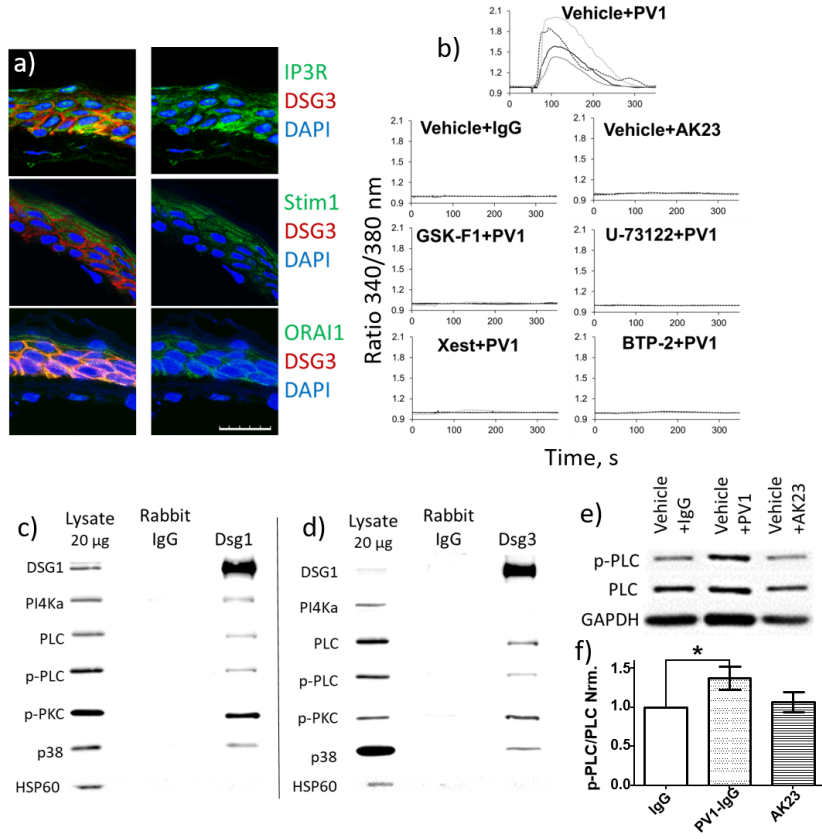
IgG name	ELISA score for anti- <i>DSG1</i> -IgG, U/ml	ELISA score for anti- <i>DSG3</i> -IgG, U/ml
PV1	1207.00	3906.00
PV2	57.60	177.00
PV3	981.00	698.00

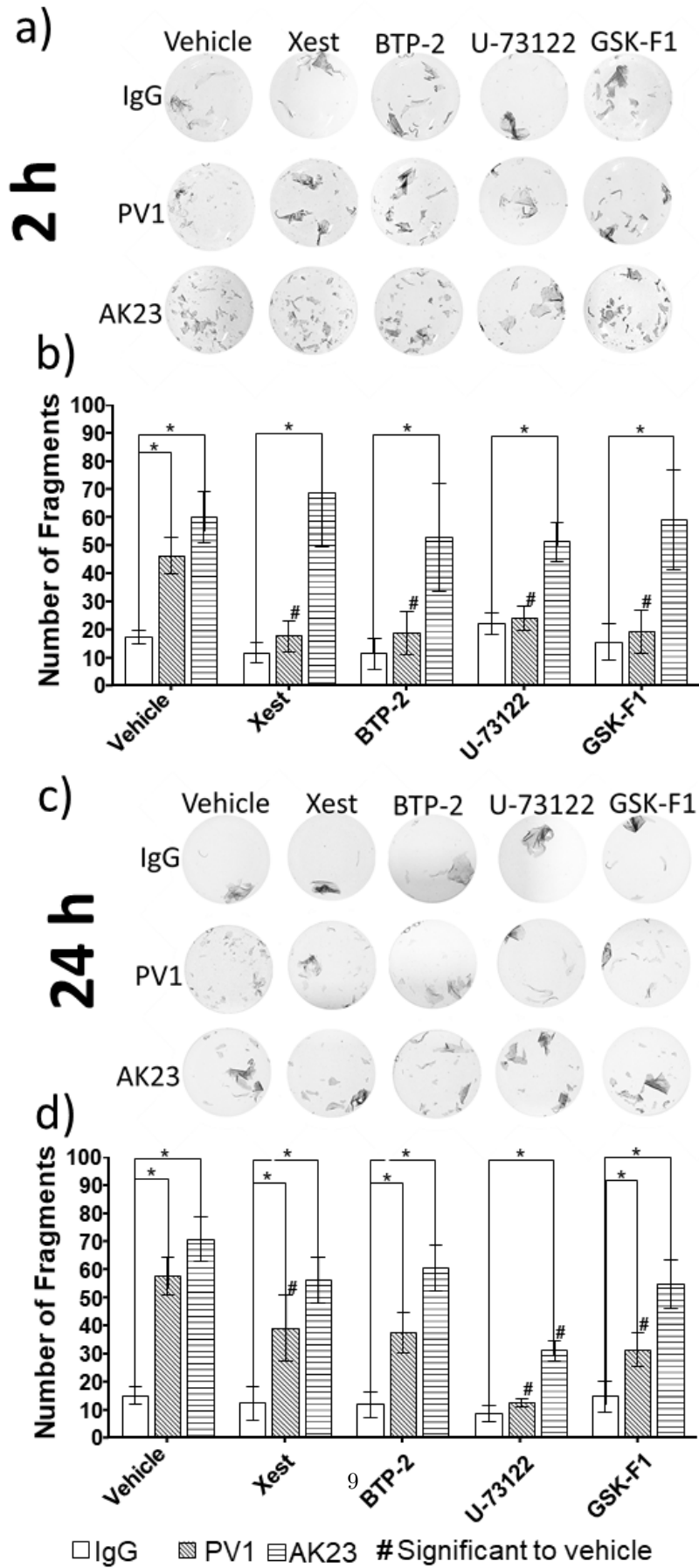
Figure 1: a) Immunostaining of Ca^{2+} channel proteins in human skin sections (n=3, scale bar 25 μm). b) Ca^{2+} flux measurements upon IgG addition performed using FURA-2-AM in NHEK cells. Each curve represents 1 independent experiment, showing an average of 8 individual randomly selected measured cells, occasional non-responding cells were not included (n=4). c) Co-immunoprecipitation experiments using NHEK cells, precipitating with anti-*DSG 1*-IgG (n[?]3). d) Co-immunoprecipitation experiments using NHEK cells, precipitating with anti-*DSG 3*-IgG (n[?]3). e) Representative Western blot showing the phosphorylation of *PLC* after 2 h IgG treatment. f) Quantification of *PLC* phosphorylation in Western blot after 2 h IgG treatment (n=6).

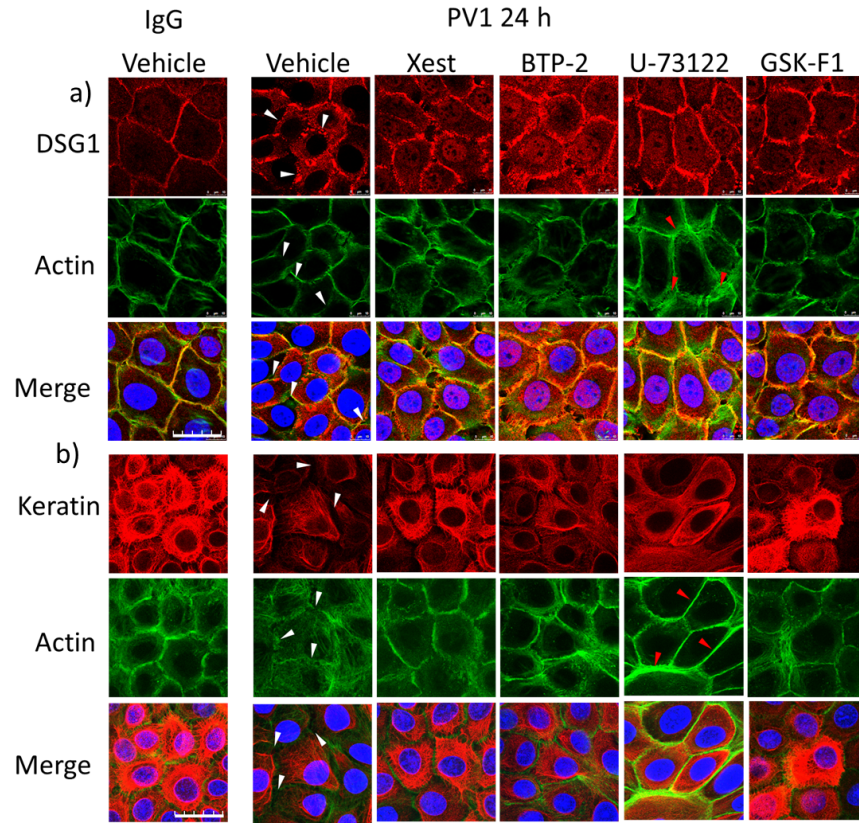
Figure 3: a) Immunostaining of *DSG 1* (rabbit-pAb, Abclonal, USA) in NHEK cells. c) Immunostaining of keratin filaments in NHEK cells. White arrows: PV-IgG-induced fragmentation of *DSG 1* staining or keratin and actin reorganization after incubation for 24 h; red arrows: strengthening of the cortical actin (n[?]3, scale bar 25 μm).

Figure 4: a) Quantitative evaluation of blister formation in human skin slices ex vivo. b) Representative microscopic images of HE staining of human skin slices after IgG treatment for 24 h (n=3). c) Immunostaining of *DSG 1* (mouse-mAb, Progen, Germany) in human skin slices after PV2 treatment. d) F-actin staining in human skin slices after PV2 treatment. Each set of images shows a 4x zoom of the blister roof and bottom. Green arrows: Missing staining at the cell border; White arrows: Remaining basal cells (tombstoning) with reduced staining (n=3, scale bar=50 μm).

Figure 5 : Schematic of the Ca^{2+} flux-dependent signalling pathway in keratinocytes upon PV-IgG binding.





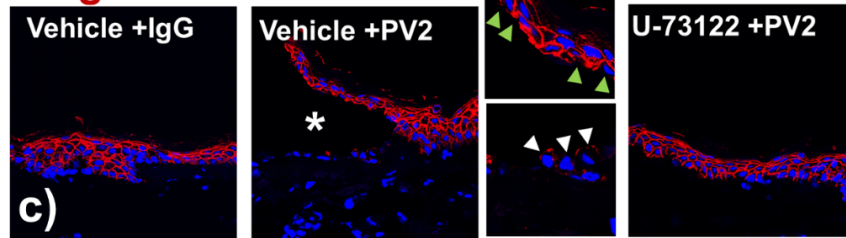


a)	IgG				
	Max rel. cleft leigth	Tot. rel. cleft length	Max cleft length	total cleft length	Nr. of Blisters
Vehicle	0	0	0 μm	0 \pm 0 μM	none
U-73122	0	0	0 μm	0 \pm 0 μM	none
	PV2				
	Max rel. cleft leigth	Tot. rel. cleft length	Max cleft length	total cleft length	Nr. of Blisters
Vehicle	22.4 %	14 \pm 1 %	904.21 μm	660.29 \pm 202.81 μM	2-5
U-73122	0	0	0 μm	0 \pm 0 μM	none

H&E



Dsg1



Actin

